JOURNAL OF CHEMICAL INFORMATION AND MODELING

Article

pubs.acs.org/jcim

Computer-Aided Structure-Based Design of Multitarget Leads for Alzheimer's Disease

José L. Domínguez,[†] Fernando Fernández-Nieto,[‡] Marian Castro,[§] Marco Catto,[∥] M. Rita Paleo,[†,‡] Silvia Porto,[‡] F. Javier Sardina,[‡] José M. Brea,[§] Angelo Carotti,[∥] M. Carmen Villaverde,*[,†] and Fredy Sussman*[,†]

[†]Departamento de Química Orgánica, Facultad de Química, Universidad de Santiago de Compostela, 15782 Santiago de Compostela, Spain

[‡]Centro Singular de Investigación en Química Biológica y Materiales Moleculares (CIQUS), Universidad de Santiago de Compostela, 15782 Santiago de Compostela, Spain

[§]Departamento de Farmacología, Instituto de Farmacia Industrial, Centro de Investigación en Medicina Molecular y Enfermedades Crónicas (CIMUS), Universidad de Santiago de Compostela, 15782 Santiago de Compostela, Spain

[∥]Dipartimento di Farmacia-Scienze del Farmaco, Università degli Studi di Bari "Aldo Moro", 70125 Bari, Italy

Supporting Information

ABSTRACT: Alzheimer's disease is a neurodegenerative pathology with unmet clinical needs. A highly desirable approach to this syndrome would be to find a single lead that could bind to some or all of the selected biomolecules that participate in the amyloid cascade, the most accepted route for Alzheimer disease genesis. In order to circumvent the challenge posed by the sizable differences in the binding sites of the molecular targets, we propose a computer-assisted protocol based on a pharmacophore and a set of required interactions with the targets that allows for the automated screening of candidates. We used a combination of docking and molecular dynamics protocols in order to discard nonbinders, optimize the best candidates, and provide a rationale for their potential as inhibitors. To provide a proof of concept, we proceeded to screen the literature and databases, a task that allowed us to identify a set of carbazole-containing compounds that initially showed affinity only for the cholinergic targets in our experimental assays. Two cycles of design based on our protocol led to a new set of analogues that were synthesized and assayed. The assay results revealed that the designed inhibitors had improved affinities for BACE-1 by more than 3 orders of magnitude and also displayed amyloid aggregation inhibition and affinity for AChE and BuChE, a result that led us to a group of multitarget amyloid cascade inhibitors that also could have a positive effect at the cholinergic level.

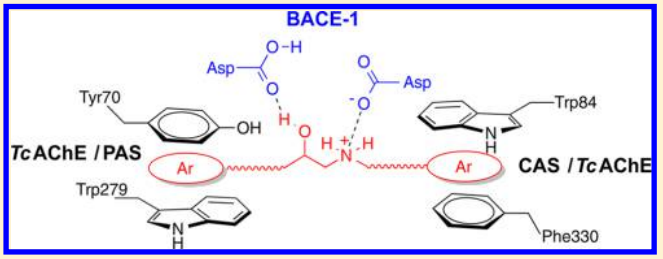

INTRODUCTION

Alzheimer's disease (AD), a cerebral neurodegenerative pathology that is the main cause of dementia in older people, is characterized by the progressive formation of insoluble amyloid plaques and fibrillary tangles. In spite of the enormous efforts carried out by academic institutions and the pharmaceutical industry, AD is an illness with unmet needs since the only drugs available in clinic (i.e., acetylcholinesterase (AChE) inhibitors and an NMDA receptor antagonist) have a palliative effect and do not modify the course of the disease.[1]

The most accepted hypothesis for the origin of AD is the one related to the amyloid cascade, which singles out aggregates and fibrils of the amyloid peptide (Aβ, a peptide of 40 or 42 residues) as the cause of AD, since their presence interrupts the synaptic connections and precludes the right interneuron orientation.[2,3] The Aβ peptides are produced by hydrolysis of the amyloid precursor protein (APP) by two aspartic proteases (γ-secretase and BACE-1). The past decade has witnessed an all-out effort to discover inhibitors of these two enzymes that could become drug leads for the treatment of AD, but all of the candidates have failed at either preclinical or clinical stages.[3] The inhibition of Aβ peptide aggregation has become an important target for drug lead discovery in itself, although no Aβ aggregation inhibitor has surpassed the clinical assays either.[1] On the other hand, Inestrosa et al.[4] have shown that the peripheral anionic site (PAS) in AChE could be a therapeutic target, since it is a nucleation site for amyloid Aβ peptide aggregation and hence its inhibition could hinder this process. Finally, leads that bind AChE could also bind butyrylcholinesterase (BuChE) and hence have a bearing on the cholinergic pathway by precluding the hydrolysis of acetylcholine and probably enhancing (albeit temporarily) cognition in AD patients.

The multiplicity of amyloid cascade AD targets (described above) opens the door to a new approach toward single-molecule polypharmacology that entails the search for a molecule that

Received: September 12, 2014
Published: December 7, 2014

ACS Publications © 2014 American Chemical Society

DOI: 10.1021/ci500555g
J. Chem. Inf. Model. 2015, 55, 135−148

could bind to all or some of the selected amyloid cascade targets. This novel paradigm, which deviates radically from the one target, one molecule strategy, has recently received increasing attention.[5−7] Probably the major hurdle in the search for multitarget leads lies in the substantial structural and specificity differences among the binding sites of the amyloid cascade targets, which drastically hinder this therapeutic strategy.[6] These differences are especially noticeable between BACE-1 and the other amyloid cascade targets such as AChE and Aβ peptide aggregation. It has been shown that the compounds aimed at these latter targets share some common traits (e.g., the presence of aromatic moieties), an issue that explains the large body of work on this multitarget subset.[7] It would be desirable to find a systematic computer-assisted protocol leading to compounds that bind to the selected set of targets. Herein we postulate the existence of a pharmacophore for a multitarget approach to AD that bears some of the traits of the known leads that bind a variety of amyloid cascade targets.[5−7] This pharmacophore could be used for a systematic search of novel multitarget leads. As a proof of concept, it has enabled us to identify in the literature some candidates bearing the requirements of our proposed structural framework.[8] Nevertheless, the results of our experimental binding assays indicate that although these compounds bind AChE, they exhibit modest fibril formation inhibition and display much lower affinities for BACE-1. Our main endeavor in this work was to generate congeneric ligands with better affinities for all of the amyloid cascade targets selected here. For this sake, we developed a protocol that relies on molecular-docking-based screening for the enzyme targets and molecular dynamics (MD) simulations for peptide aggregation in order to search for more potent analogues of our starting candidates. The main novelty of the protocol elaborated by us is that it allows a systematic search of multitarget leads and their subsequent optimization, given the fact that our hit docking poses should comply with the set of inhibitor−protein interactions assigned to our pharmacophore. Review of the predicted docking poses in AChE and BACE-1 revealed possible ways of enhancing binding affinity. Two cycles of design based on our protocol led to a new set of analogues that were synthesized and assayed. The assay results revealed that the designed inhibitors had improved affinities for BACE-1 by more than 3 orders of magnitude and also displayed affinity for amyloid aggregates, AChE, and BuChE, a result that led us to a group of truly multitarget candidates that interrupt the amyloid cascade while having a positive effect at the cholinergic level.

Furthermore, our results allowed us to explore some basic questions that relate to molecular recognition issues in the different amyloid cascade targets, including the charge state of the BACE-1 main anchoring group and the mechanism by which the best leads may interrupt the amyloid peptide aggregation.

Multitarget Amyloid Cascade Pharmacophore. Our pharmacophore was built by identifying the specific moieties that are recognized by the binding pockets of the different amyloid cascade targets. For instance, an essential feature in BACE-1 inhibitors is a functional group (e.g., hydroxyethylene, hydroxyethylamine, guanidium, etc.) that can interact through hydrogen bonds and ion pairs with the Asp dyad, the catalytic machinery of this enzyme.[9] Our choice for this kind of functionality was based on recent studies in our lab that identified the hydroxyethylamine group as an Asp dyad anchor that favors good performance at cellular level.[10,11] On the other hand, an overview of the AChE inhibitors indicates that many of them contain one or two aromatic moieties that interact through π-stacking interactions with clusters of aromatic residues present in both the catalytic anionic site (CAS) and the PAS.[12] The two AChE binding sites are separated by a long gorge. Hence, our ideal AChE inhibitor should include an optimum-length spacer that connects the aromatic moiety residing in the CAS with the one at the PAS. If we accomplish this aim, the resulting lead should have both a palliative effect on AD and hinder amyloid aggregation. Finally, some of the amyloid aggregation inhibitors share with the AChE ligands a common feature, namely, the presence of aromatic groups that target some of the residue clusters rich in aromatic residues present in the amyloid peptide (such as the LVFFA segment). Hence, a multitarget pharmacophore and its possible interactions in the amyloid cascade binding sites could be described by a scheme such as the one presented in Figure 1. A number of the features that appear

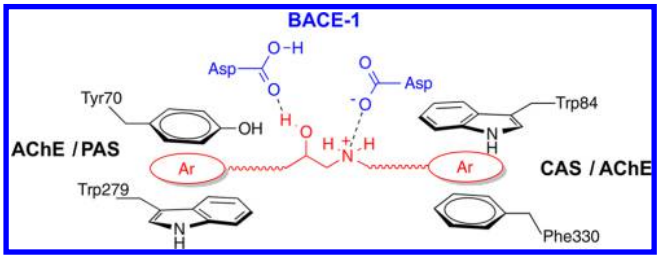

Figure 1. Schematic view of our multitarget pharmacophore (red) bound to the Asp dyad of BACE-1 (blue) and to the CAS and PAS of *Tc*AChE (black).

in this pharmacophore have been used in the search for multitarget cascade leads.[5−7] Herein we demonstrate that the described pharmacophore could be used for multitarget screening and subsequent lead optimization.

The computer-assisted search for candidates based on the pharmacophore shown in Figure 1 led us to find some compounds **1** (see Figure 2) with neurogenerative and

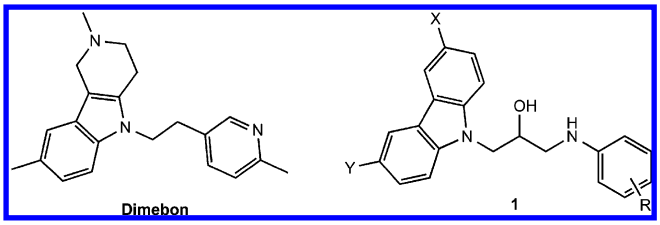

Figure 2. Structure of dimebon and the analogues **1** selected for this work.

neuroprotective properties in mice.[8] Nevertheless, the molecular therapeutic targets for these compounds have not been identified. The stated aim of the study that led to these compounds in the first place was to find analogues of dimebon, a carbazole derivative that in itself showed good promise in AD assays in animals but failed in phase-3 clinical trials.[13] Moreover, other carbazole derivatives have been shown to be good Aβ aggregation inhibitors.[14] As shown by structure **1** in Figure 2, these compounds present all of the structural features that make them good leads for all amyloid cascade targets. On one hand the hydroxyethylamine moiety provides an anchor for BACE-1 binding, while the aromatic moieties on both ends (carbazole and substituted phenyl groups) could be a source of affinity of these compounds for AChE and Aβ peptide oligomers. On the basis of this information, we decided to investigate whether the original group of compounds **1** owed their beneficial properties at the

DOI: 10.1021/ci500555g
J. Chem. Inf. Model. 2015, 55, 135−148

central nervous system level to their binding to some of the amyloid cascade targets and whether we could produce analogues with better affinity for a wider range of amyloid cascade targets.

COMPUTATIONAL METHODS

Pharmacophore-Based Candidate Search. The quest for compounds bearing the traits of the pharmacophore was performed using the SMILES structure descriptors on bibliographical databases. A variety of different structures were identified, some of them bearing a hydroxyethylamine and others bearing unwanted fragments such as amino ketones. The unwanted candidates were pruned by using a simple AWK script.

Docking Protocols. We carried out the docking simulations with the suite of modules resident in the program GOLD.[15] For each docking run, we employed a minimum of 100 000 and a maximum of 1 250 000 genetic generated poses. We scored the poses with three of the scoring functions resident in GOLD (i.e., GoldScore,[16,17] ChemScore,[18−20] and ChemPLP[21]).

Docking to BACE-1. One of the most outstanding structural features of the active site of BACE-1 is a residue segment (residues 69−75) that forms a flap whose conformational variability allows for a great variety of binding poses for those inhibitors differing in size and shape.[9] This loop, which forms part of the S1 pocket, closes in on the active site during substrate catalysis. There are inhibitors that bind explicitly to the flap, preventing its closure and hence hampering catalysis. Perusal of the many BACE-1−inhibitor complex structures indicates that the flap presents a wide variety of openings depending on the inhibitor's chemical nature. In order to take the flap variability into account in our docking calculations, we carried out our docking simulations with three protein templates that differ in the opening of this loop. The first of these protein structures comes from the complex between BACE-1 and the peptidemimetic inhibitor **OM99-2** (PDB entry 1FKN) and has a closed flap.[22] The second structure has a non-peptidic inhibitor bound to the enzyme with a middle-range opening of the flap (PDB entry 3KMY),[23] while the last template was obtained from the unbound structure of BACE-1 and has a fully opened flap (PDB entry 1W50).[24] Figure 3 shows a superposition of these three structures with the flap structures displayed in different colors.

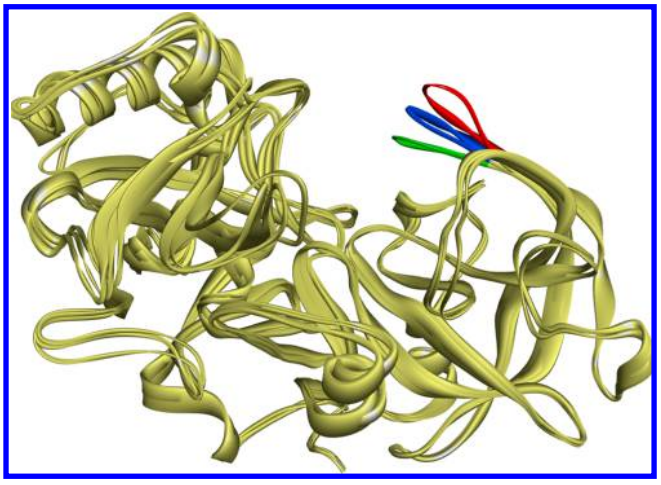

Figure 3. Superimposition of the 1FKN, 3KMY, and 1W50 protein ribbon structures. The flap loops are colored in green, blue, and red, respectively.

Our previous studies, which combined surface plasmon resonance binding experiments with molecular-mechanics-based calculations, predicted that the Asp dyad in BACE-1 has a monoprotonated state (at pH values ranging from 4.5 to 7.4) when bound to compounds with a hydroxyethylamine moiety.[10] Thus, we assigned this Asp dyad state to BACE-1 in our docking screening calculations. On the other hand, the aniline present in our compounds could be protonated or neutral at the acidic pH (4.5−5.0) at which the experimental assays were carried out. For this reason, docking simulations for these compounds were carried out both with neutral and protonated anilines.

As a first step, we cleaned up the target structures mentioned above by eliminating the crystallographic water molecules, discarding alternative conformations, and adding hydrogen atoms using the Discovery Studio (DS) modules.[25] We defined the targeted binding site for GOLD docking to these proteins as all of the atom residues within 6 Å of the inhibitor in the 3KMY complex.

For each of the structures differing in the flap opening, we then performed docking calculations with one of the three scoring functions (ChemScore, GoldScore, and ChemPLP). In each of the runs, we searched for the presence of a single hit pose among the top 10 resulting docking poses. We defined a hit pose as one that fulfills the hydrogen-bonding pattern between the hydroxyethylamine fragment and the Asp dyad shown for our pharmacophore in Figure 1. Global success rates for every candidate compound were calculated by adding up the numbers of single hits of the docking simulations carried out with the three scoring functions for our three protein templates differing in the flap opening described above.

Docking to AChE. For the docking predictions to this target, we used the X-ray structure of *Torpedo californica* (*Tc*AChE) complexed with a bis(8)-tacrine analogue (PDB entry 1ODC).[26] A close-up of the binding pose is shown in Figure 4. In the same

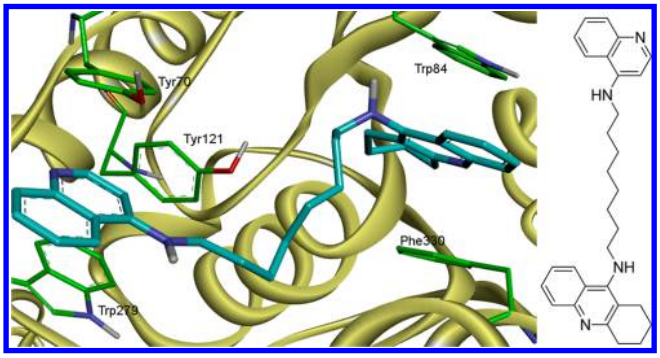

Figure 4. Close-up of the binding of the indicated bis(8)-tacrine analogue to both binding sites (CAS and PAS) in *Tc*AChE (from PDB entry 1ODC). The inhibitor is shown in blue, and the aromatic residues are shown in green. The $\pi-\pi$ interactions of the aromatic moieties with the side chains of residues Trp 84 and Phe 330 at the CAS and with residues Tyr 70 and Trp 279 at the PAS should be noted.

way as for BACE-1, we cleaned up the target structure (PDB entry 1ODC) by eliminating the crystallographic water molecules, discarding alternative conformations, and adding hydrogen atoms using the DS modules.[25] We defined the binding site as all of the AChE atom residues that lay at 6 Å from the ligand of this complex (i.e., the bis(8)-tacrine analogue). Again, the docking conformations generated by the genetic algorithm were evaluated using the same scoring functions as for BACE-1. In each run, the top 10 poses were screened for compliance with

DOI: 10.1021/ci500555g
J. Chem. Inf. Model. 2015, 55, 135−148

the face-to-face π-stacking interactions that optimize the inhibitor affinity at both the CAS and PAS in AChE, as shown in Figure 1 and exemplified by the bis(8)-tacrine analogue in Figure 4. In the same way as in BACE-1, the hit success rate was determined by searching for a hit among the top 10 poses for the docking simulations evaluated with our three scoring functions. Global success rates were calculated by adding up the numbers of single hits.

Aβ Aggregation Inhibition Protocol. As we explained in the Introduction, one of the therapeutic targets is inhibition of the Aβ peptide oligomerization that leads to the neuronal toxic species. These peptides do not have a unique binding site for the ligands as in the case of other AD amyloid cascade enzymatic targets. Depending on the nature of the ligand, there are multiple binding sites that share similar sequence motifs. For instance, some aromatic moiety inhibitors tend to bind to aromatic residue clusters present in the LVFFA segment of the amyloid peptide.[27] Hence, many in silico aggregation inhibition studies merge docking protocols with MD simulations.[28] We explored a different approach recently developed by the group of Caflisch.[27a] It consists of analyzing lengthy MD simulations of a segment of the Aβ peptide (Aβ12−28) in the presence of a given candidate. This peptide fragment was chosen for several reasons. First, the initial 11 residues were omitted since they lack any definite secondary structure in some NMR amyloid aggregate structures.[29] Moreover, the selected segment contains one of the regions (LVFFA) around which a β-hairpin (the template for Aβ aggregation) forms and is also one of the ligand's binding spots for a number of ligands.[27] Finally, this segment has been used in NMR-based experiments to study ligand binding locations.[27b]

Our extensive MD calculations were carried out with the CHARMM PARAM-19 force field,[30] which employs an extended atom approximation for all carbon atoms. Protonation states of all titratable residues were considered at neutral pH. In particular, the side chains of the His residues were assigned a neutral charge, whereas the basic residues (Arg/Lys) and the acidic residues (Asp/Glu) were assigned positive and negative charges, respectively. We used an implicit solvation protocol called fast analytical continuum treatment of solvent (FACTS), an efficient generalized Born (GB) implicit solvation model developed by Caflisch's group,[31] which includes a solvent-accessible surface of the solute for the nonpolar contribution.

MD simulations were carried out with periodic boundary conditions at a fixed peptide concentration of 2.5 mM (87 Å cubic simulation box) using the Langevin integrator at low friction (coefficient of 0.15 ps^{-1}) and a temperature of 300 K. Using a time step of 2 fs, for each system we performed five independent runs that added up to a 5 μs trajectory. Each of the starting structures contained the peptide in an extended conformation together with the inhibitor candidate in a different position. As a reference, we used simulations of the peptide with the known aggregation inhibitor 9,10-anthraquinone and of the ligand-free peptide. The initial structures were subjected to two energy minimization runs, which began with a 500-step steepest descent run followed by a 50000-step conjugate gradient calculation. In each case, the gradient tolerance was 0.001 kcal·mol^{-1}·$Å^{-2}$. Then a 0.5 ns heating stage and a 0.5 ns thermal MD equilibration stage were carried out, followed by the production stage described above.

Since every MD simulation took 1 month of wall-clock computer time, we had to select the kind and number of compounds used in our calculations. For instance, for the indole derivatives we performed simulations on only one aniline- and two benzylamine-containing compounds (see below). Our simulations were then used to calculate the average residence times of the ligand around the peptide and around every residue of the peptide as well as the effect of the ligand on the secondary structure of the peptide. The statistical significance of these results is provided by the standard deviations based on the individual trajectories.

RESULTS

1. First Lead Optimization: Carbazole Derivatives. *1.1. BACE-1 Ligand Screening.* The first set of compounds studied were the carbazole derivatives bearing an aniline moiety with a substituent at either the ortho or meta position that originally showed neuroprotective and neurogenerative activity in mice.[8] From this study we chose a subset whose chemical structures and docking data are displayed in Table S1 in the Supporting Information, while the global docking success rates (see Computational Methods for details) are shown in Figure 5.

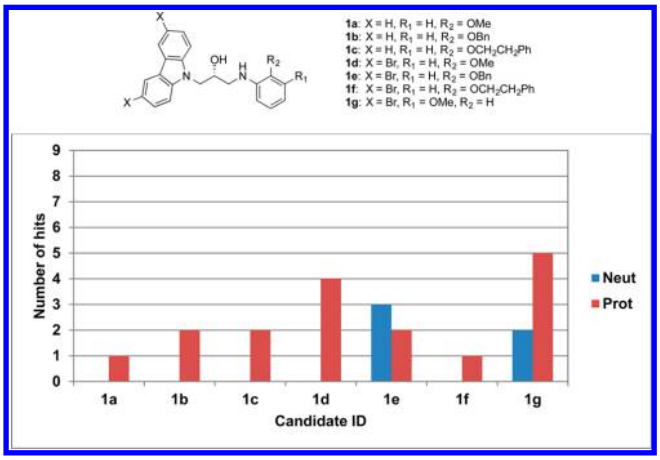

Figure 5. Global BACE-1 docking success rates of aniline-substitued ligands as provided by the numbers of single hits across flap openings and docking scoring functions. Neut and Prot indicate neutral and protonated ligands, respectively.

As can be seen from Figure 5 and Table S1, the compounds that have a methoxy substituent on the aniline at either the ortho position (compound **1d**) or the meta position (compound **1g**) are the ones that show the widest consensus as possible BACE-1 inhibitors. The better fit displayed by these compounds could be the result of reduced steric clashes, as they are the smallest candidates in this list. For the same reason, our predictions indicate that the smaller ligands bind to BACE-1 with any of the three flap openings (see Table S1). Nevertheless, given their size, it is doubtful that these ligands could span both the CAS and PAS in AChE and hence become multitarget leads.

Perusal of the results in Figure 5 and Table S1 shows that the available hits were obtained almost exclusively when the docking calculations were carried out with a charged ligand. Actually, only two of the seven compounds (**1e** and **1g**) displayed some hits when neutral. This result is in line with our previous studies,[32] which indicate that there is an enrichment in the number of predicted poses close to those observed experimentally when the ligand is charged.

The pK_a of the protonated amino group belonging to the aniline moiety for these compounds in solution is ca. 4.7, a value that is close to the pH at which the binding assays were

DOI: 10.1021/ci500555g
J. Chem. Inf. Model. 2015, 55, 135−148

performed. Replacing the aniline by a benzylamine moiety was expected to increase the pK_a of the protonated amino group and hence the likelihood that it would be charged, an outcome that should boost the number of predicted BACE-1 binders. Figure 6

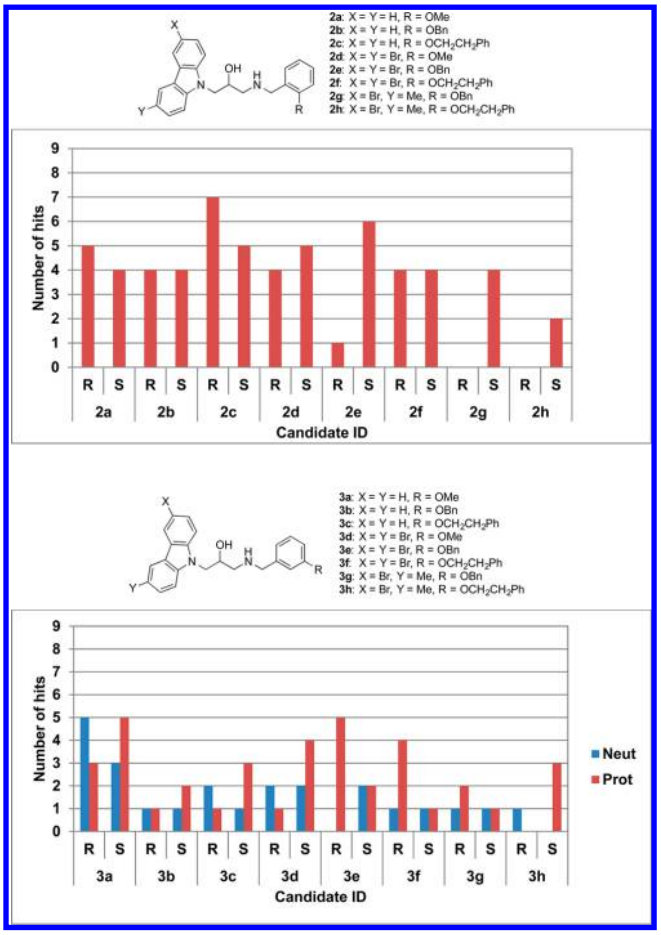

Figure 6. Global hit success resulting from the docking to BACE-1 of (top) protonated ortho-substituted benzylamines and (bottom) both neutral and protonated meta-substituted benzylamines. R and S indicate the two possible enantiomeric configurations of each compound.

displays the global hit success for benzylamine-containing compounds substituted at the ortho position (upper panel) or the meta position (lower panel). The detailed data for these docking calculations are shown in Tables S2 and S3. Comparison of the number of single hits among the top 10 exit poses for analogous aniline (Table S1 and Figure 5) and benzylamine (Tables S2 and S3 and Figure 6) compounds indicates a substantial increase in the hit rates for benzylamines above those calculated for the aniline-containing compounds, an outcome that validates our design premises.

Perusal of Figure 6 indicates that the benzylamine substitution pattern also has a bearing on the number of possible hits. The results would seem to indicate that ortho substitution is favored over meta substitution on the benzylamine moiety. For instance, among the top 10 poses, the number of single hits with ortho substitution is twice the number of hits with meta substitution (see Tables S2 and S3). Nevertheless, there seem to be exceptions (e.g., see compound **3e** when the hydroxyl group is in the *R* configuration) that had a number of hits comparable to those for the analogous ortho derivatives (e.g., compound **2e** when the hydroxyl group is in the *S* configuration).

For the compounds bearing a benzylamine fragment we also analyzed the effectiveness of each stereoisomer. The results presented in Figure 6 do not show a clear predilection for a given enantiomer, as changes at the end points of the candidate compounds seem to change the preference. For instance, in the case of the compounds containing meta-substituted benzylamines, those compounds bearing two Br atoms on the carbazole favor the *R* configuration (compounds **3e** and **3f**), while those with no substituents favor the *S* configuration. Nevertheless, these configuration patterns do not seem to hold for the ortho-substituted benzylamine-bearing compounds.

1.2. AChE Ligand Screening. Figure 7 displays the AChE global hit rates for protonated anilines and benzylamines

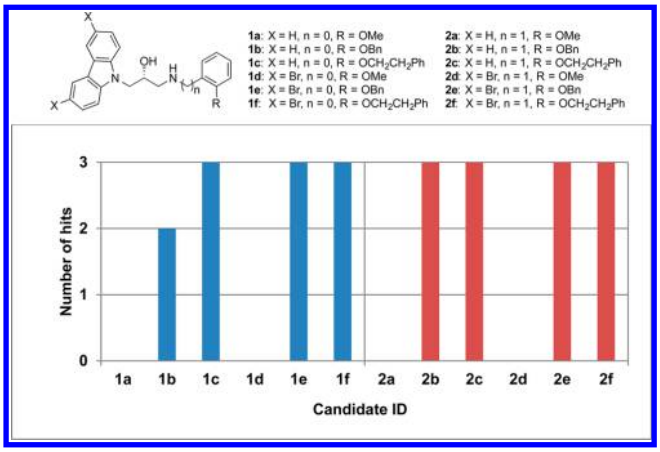

Figure 7. Global hit rates resulting from the AChE docking screening of the protonated ortho-substituted anilines (left) and benzylamines (right). The hit search was carried out among the top 10 poses resulting from three docking calculations, each carried out with a different scoring function (ChemScore, GoldScore, or ChemPLP).

substituted at the ortho position, while Figure 8 depicts the number of hits for the compounds bearing meta-substituted benzylamines. As these figures show, there is a wide consensus among the scoring function results, indicating that these

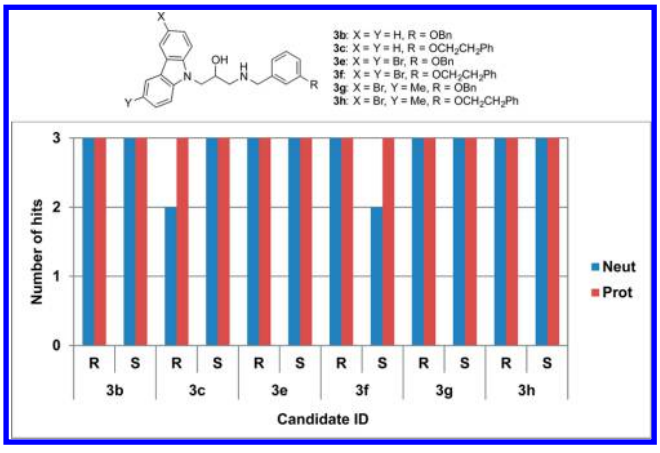

Figure 8. Global hit rates resulting from the AChE docking screening of the compounds with a meta-substituted benzylamine. For each molecule, we studied the effect of the stereochemistry of the hydroxyl group (*R* or *S*) and the protonation state of the amine group. The hit search was carried out among the top 10 poses resulting from three docking calculations, each carried out with a different scoring function (ChemScore, GoldScore, or ChemPLP).

DOI: 10.1021/ci500555g
J. Chem. Inf. Model. 2015, 55, 135−148

compounds are good candidates for AChE inhibitors, in most cases independently of the stereochemistry of the hydroxyl group and the charge of the hydroxyethylamino group. Comparison with the BACE-1 docking results described above indicates that the number of predicted hits for AChE are substantially larger than those for BACE-1, implying that there are fewer hurdles for finding a candidate that will fulfill the pharmacophore requirements for the former enzyme.

The scoring function values for aniline- and benzylamine-containing compounds are listed in Tables S4 and S5. Perusal of Table S4 and Figure 7 indicates that the shorter compounds, such as **1a**, **1d**, **2a** and **2d** (those bearing a methoxy substituent), have no hits according to our pharmacophore definition shown in Figure 1. Scrutiny of the binding pose for a methoxy-substituted compound compared with that for a benzyloxy-substituted compound (Figure 9) indicates that the former

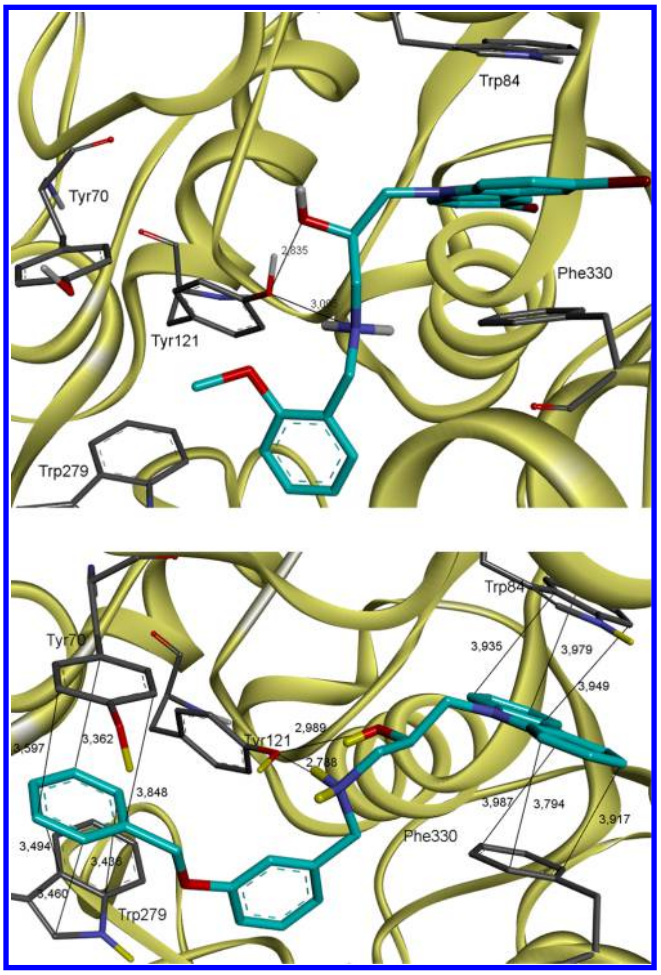

Figure 9. Docking of compounds **2d** (top) and **3b** (bottom) into AChE.

ligands derive their worse performance from their inability to bind to both the CAS and PAS in AChE. As shown in Figure 9, the carbazole moiety interacts with residues Tyr 84 and Phe 330 in the CAS through π-stacking interactions. The shorter ligand is not able to reach the PAS in AChE and hence cannot generate these types of interactions with Tyr 70 and Trp 279.

1.3. Aβ12−28 Peptide Interaction Inhibition Results. Table 1 lists the percentage residence times for 9,10-anthraquinone (a reference compound) and for some carbazole-containing compounds up to 7.5 Å from the peptide. We also calculated the residence times of these ligands around every residue of the

Table 1. Percentage Residence Times for Peptide−Ligand Contacts up to 7.5 Å

candidate	contact time (%)
1a	85 ± 2.6
1b	93 ± 0.6
1c	90 ± 2.0
1d	99 ± 0.4
1f	99 ± 0.2
anthraquinone	36 ± 1.5

peptide with a cutoff distance of 4.5 Å (see Figure 10) and the residue−residue interactions in the absence or presence of the

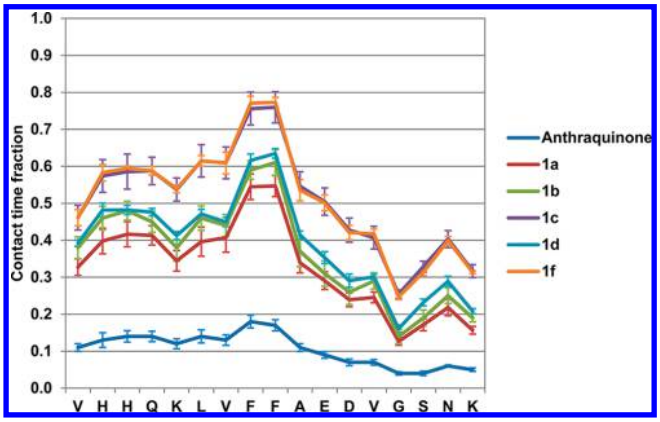

Figure 10. Ligand−peptide residue contact time fractions. The cutoff distance was set at 4.5 Å.

ligands (see Figure 11 and Figure S4 in the Supporting Information). As shown in Table 1, the candidate compounds have much larger residence times than the reference ligand. Moreover, the selected compounds display a bigger preference (compared with the reference compound) for the binding hot spots centered on both the His cluster at the N-terminal end and the aromatic cluster found at the LVFFA segment (Figure 10).

An important issue is the effect of the ligand on the secondary structure of the peptide. The Aβ peptide, which originates from APP hydrolysis, originally adopts a helix structure. As amyloid aggregates are formed, there is a change of conformation that leads to a β-hairpin, specifically around the DVGS motif. For instance, the NMR structure of a pentamer[29] clearly shows that the peptides organize themselves to form hairpins that aggregate as sheets. As shown in Figures 11 and S4, the ligands would seem to partially preclude the formation of this secondary structure motif (turn) in a monomer, a process that may lead to reduced aggregation. Hence, it may be surmised that the residue−residue contact map in the presence of a ligand may give us a measure of the aggregation inhibition effect of our candidates.

1.4. Synthesis and Experimental Assays for Carbazole-Containing Compounds. The synthesis of several carbazole-containing compounds was carried out following Scheme 1, which includes the list of synthesized molecules. Carbazole−epoxides **10** were prepared as described in the literature from carbazoles **8** and epichlorohydrin (**9**).[8,33] Regioselective ring opening of epoxides **10** with different ortho-substituted anilines **11** in the presence of $Mg(ClO_4)_2$ in acetonitrile[34] afforded carbazole compounds **1** in moderate to good yields. Similarly, as shown in Scheme 1, carbazole analogues **3** were synthesized by ring opening of carbazole−epoxides **10** with meta-substituted benzylamines **12**. The choice of compounds was guided in many

DOI: 10.1021/ci500555g
J. Chem. Inf. Model. 2015, 55, 135−148

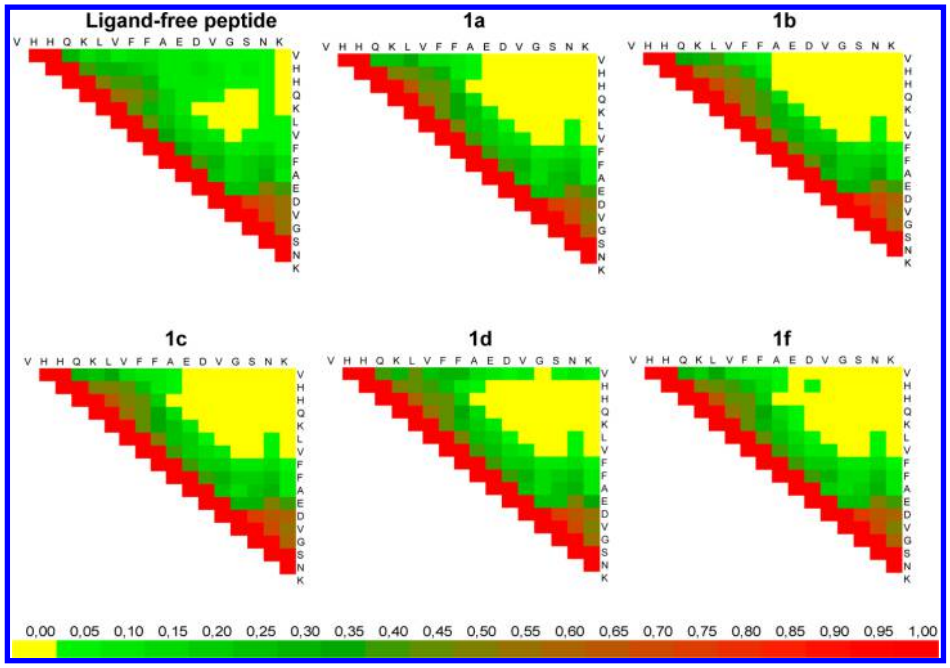

Figure 11. Residue−residue contact maps in the absence (top-left panel) or presence of inhibitors. The cutoff interaction distance was set at 4.5 Å. The color scale shown at the bottom indicates the residence time fractions.

Scheme 1. Synthetic Routes and Carbazole Derivatives Synthesized

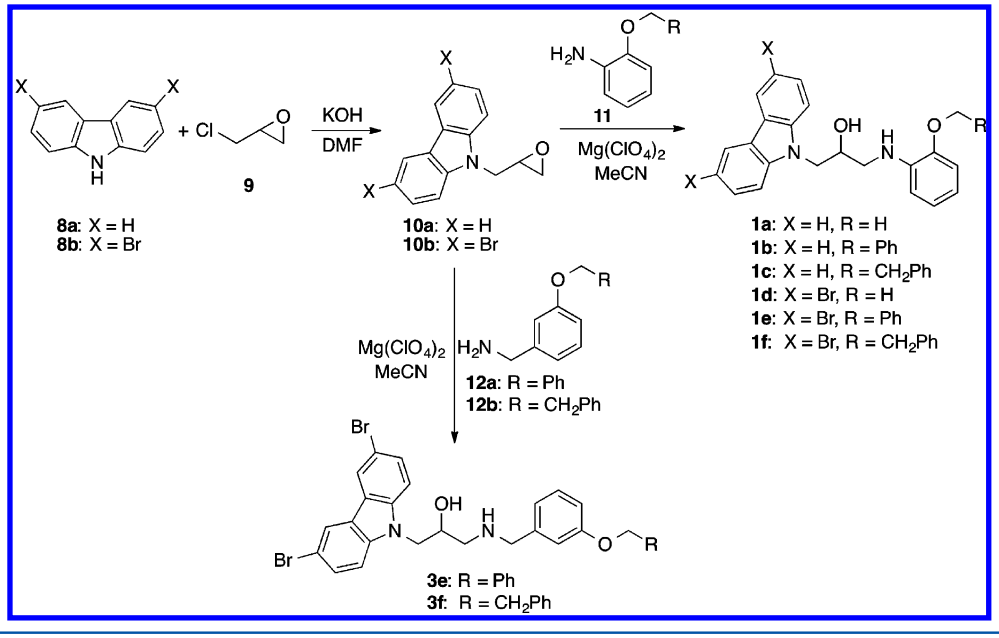

Table 2. Experimental Results of the Multitarget Assays

	*Ee*AChE		hsBuChE		Aβ(1−40)	BACE-1	
compound	% Inh. @ 10 μM	IC_{50} (μM)	% Inh. @ 10 μM	IC_{50} (μM)	% Inh. @ 100 μM	% Inh. @ 100 μM	IC_{50} (μM)
1a	30 ± 1	–	–	6.0 ± 1.0	58 ± 2	1.3 ± 0.3	–
1b	22 ± 1	–	34 ± 1	–	51 ± 5	2.4 ± 1.4	–
1c	49 ± 2	–	33 ± 1	–	36 ± 5	1.5 ± 0.3	–
1d	15 ± 1	–	12 ± 1	–	41 ± 3	1.6 ± 1.5	–
1e	–	7.2 ± 0.4	20 ± 1	–	46 ± 3	0.5 ± 0.3	–
1f	–	7.8 ± 0.2	10 ± 1	–	49 ± 1	0.9 ± 0.9	–
3e	48 ± 1	–	–	1.1 ± 0.2	11 ± 3	–	3.1 ± 0.4
3f	–	14 ± 1	–	7.1 ± 0.7	28 ± 3	–	3.1 ± 0.3

DOI: 10.1021/ci500555g
J. Chem. Inf. Model. 2015, 55, 135−148

cases by the availability of the reactants. Although in the case of benzylamines the compounds with an ortho substituent seemed to show a wider consensus as BACE-1 inhibitors across all of the scoring functions (see Figure 6), they require more elaborate and expensive chemistry. For this reason, we chose the best-scoring candidates with a meta-substituted benzylamine (**3e** and **3f**).

The results of the experimental binding assays with BACE-1, AChE, and BuChE as well as the ThT Aβ aggregation inhibition assays are shown in Table 2. As shown in this table, some of the aniline-containing compounds demonstrated promise as multitarget inhibitors. For instance, compounds **1e** and **1f** displayed micromolar binding affinity for AChE and Aβ inhibition percentages of ca. 50% at 100 μM peptide concentration, values that are superior to that for 9,10-anthraquinone (30% at 100 μM).[35] On the other hand, compound **1a** displayed micromolar affinity for BuChE and 58% percent inhibition of fibril formation. Nevertheless, none of the carbazole- and aniline-containing compounds that were originally shown to be neuroprotective and neurogenerative in mice[8] resulted in multitarget leads across all of the chosen amyloid cascade targets.

Finally, this table shows that the benzylamine-bearing compounds (**3e** and **3f**) have improved affinities for BACE-1 by 3 orders of magnitude over the aniline-containing compounds. This result validates and supports the outcome of our calculations (see Figures 5 and 6), which indicate that the addition of a CH_2 fragment provides hits across the set of scoring functions used in our calculations. As mentioned before, this effect is probably due to the larger pK_a of the benzylamine's amino group, which favors the formation of an ion pair with one of the Asp residues of the active-site Asp dyad. These latter compounds (**3e** and **3f**) have improved affinity for BuChE, and **3f** also displays micromolar affinity for AChE. Nevertheless, their Aβ aggregation inhibition dropped below the 30% inhibition displayed by the reference compound (9,10-anthraquinone).

2. Screening of Third-Generation Candidates: Indole-Based Multitarget Candidates. The carbazole moiety present in the candidates synthesized and assayed above is quite a bulky group. Perusal of the resulting binding poses showed some steric clashes between the ligand and some protein side chains. The close van der Waals contacts are allowed by the GOLD docking protocol as a way of compensating for the lack of protein flexibility.[15] Figures S1 and S2 display the steric clashes of some ligands with BACE-1 and AChE. An option to avoid the steric clashes altogether would be to search for a smaller aromatic group in place of the carbazole, such as an indole. On the basis of this idea, we designed a new generation of multitarget candidates bearing this fragment at one end and the same aromatic moieties used in the previous sections (substituted anilines and benzylamines) at the other end. For these ligands we chose the OBn substituent for the anilines and benzylamines because the analysis of the results for the carbazole-containing compounds described above showed that this substituent provides leads with the right length to span the distance from the CAS to the PAS in AChE.

2.1. BACE-1 Ligand Screening. Figure 12 lists the global hit success for the indole-based derivatives, while the scoring function values for this set of compounds are listed in Tables S6 and S7. The structural variables analyzed in these figures are the same as in the study of the carbazole derivatives in the previous section and include the moiety to which the amino group belongs (aniline or benzylamine), its protonation state, the substitution of the indole group, the substituent position (ortho or meta) on the other aromatic ring, and the stereochemistry of the OH group.

Perusal of our results indicates that the indole-based ligands have a higher probability of binding to BACE-1 with a medium-open or fully open flap (see Tables S6 and S7). The number of hits with a closed flap are very small, especially when using the ChemPLP scoring function, indicating that these molecules fit in the active site of BACE-1 thanks to the plasticity of its flap.

In the case of the carbazole-based compounds, the best-ranking ones were those that contained a benzylamine moiety, the one that assured the existence of a protonated amino group. A global comparison of the indole-based compounds containing an aniline (Figure 12, top panel) with those containing a

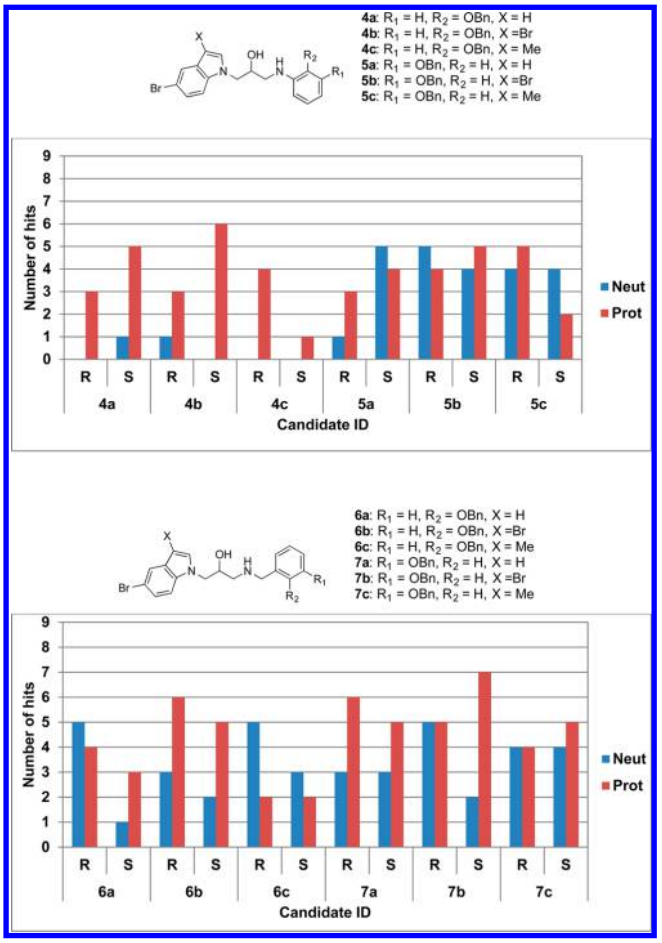

Figure 12. Global hit success resulting from the docking to BACE-1 of indole derivatives bearing (top) anilines and (bottom) benzylamines.

benzylamine (Figure 12, bottom panel) indicate that the latter present a larger global hit rate, a pattern similar to that observed for the carbazole-containing compounds. Nevertheless, the preferred benzylamine substitution pattern in the indole-based compounds predicted by our calculations differs from the one predicted for the carbazole-containing ligands, since these latter compounds favor an ortho rather than meta substitution pattern for benzylamines. On the other hand, perusal of Figure 12 suggests that the indole-based compounds favor meta over ortho substitution, a substitution pattern also followed by the aniline-bearing compounds. Moreover, for these latter compounds, the largest increase is observed for the hits containing a neutral ligand.

DOI: 10.1021/ci500555g
J. Chem. Inf. Model. 2015, 55, 135−148

We also studied the effect of the ligand protonation state on the number of hits. For both the aniline- and benzylamine-containing compounds (Figure 12), the number of hits is larger (for the most part) when the amino group is protonated rather than neutral.

2.2. AChE Ligand Screening. The global hit rate resulting from the AChE-docking-based screening calculations for the indole derivatives containing an aniline or benzylamine substituted at the ortho or meta position are depicted in Figure 13. Comparison of the effect of the substitution pattern for both aniline and benzylamine (shown in this figure) indicates that changing the substitution from ortho to meta increases the number of hits. As can be seen from Figure 13, the number of hits obtained and the consensus reached across the three scoring functions indicate that our indole- and benzylamine-containing compounds fit well inside AChE, spanning both the main site (CAS) and the peripheral one (PAS). Moreover, comparison of the aniline-bearing compounds with the benzylamine-bearing ones indicates that the latter present a larger number of hits across all three scoring functions, probably because of the increase in the size of the ligands that allows them to span the two binding sites better.

One interesting issue is the docking exit poses. As we mentioned above in our pharmacophore depiction for AChE, we seek to have dual inhibitors in which one of the end aromatic fragments is to be found at the CAS and the other end aromatic group positions itself in the PAS, both producing π-stacking interactions with the aromatic residue clusters residing in these two sites (see Figure 1). There are two possible pose orientations that fulfill this hit. In the first one, the indole moiety is predicted to be found in the CAS while the terminal benzyloxy group is to be found at the PAS. In the second possible pose, we have the inverse option in which the indole fragment resides at the PAS. In Figure 13 we have listed both poses and referred to them as "CAS" and "PAS", respectively. As shown in these plots, the number of "CAS" hits (indole docked into the CAS) is larger than those when the indole fragment is placed in the PAS for both the aniline- and benzylamine-containing compounds, a result that we will try to verify through X-ray crystallography. In Figure 14 we depict the most favored pose obtained for compound **7a** with the ChemScore fitness function. It should be noted that the indole fits neatly into the CAS, making π-stacking interactions with residues W84 and F330, while the Bn group interacts with W279 and Y70 in the PAS.

Finally, the results shown in Figure 13 indicate that there is scarcely a preference for one of the enantiomers and that there is no clear proclivity for a neutral or charged state for the amino group.

2.3. Inhibitor Aβ12−28 Peptide Interaction Results. We performed MD simulations on three of our indole candidates: one containing an aniline fragment (**4b**) and the other two containing a benzylamine moiety (**7b** and **7c**). The results indicate that the percentage residence times around the peptide with 7.5 Å radii for these compounds are relatively high (88 ± 2.0, 96 ± 2.0, and 86 ± 1.3%, respectively). Figure 15 displays the ligand residence times around every residue of Aβ12−28. As shown in this figure, the ligands favor two binding spots (populated by aromatic residues), a result already observed for the carbazole-containing compounds. The most frequented site is around the LVFFA segment, and the second one contains the two His residues at the start of the sequence. Another important feature is that these ligands present much higher residence times than the reference ligand, 9,10-anthraquinone, a compound that has a 30% fibril formation inhibition at 100 μM concentration. Furthermore, comparison of the intrapeptide residue interactions when these three ligands are present (see Figures 16 and S4) with the residue contacts when they are absent (see Figures

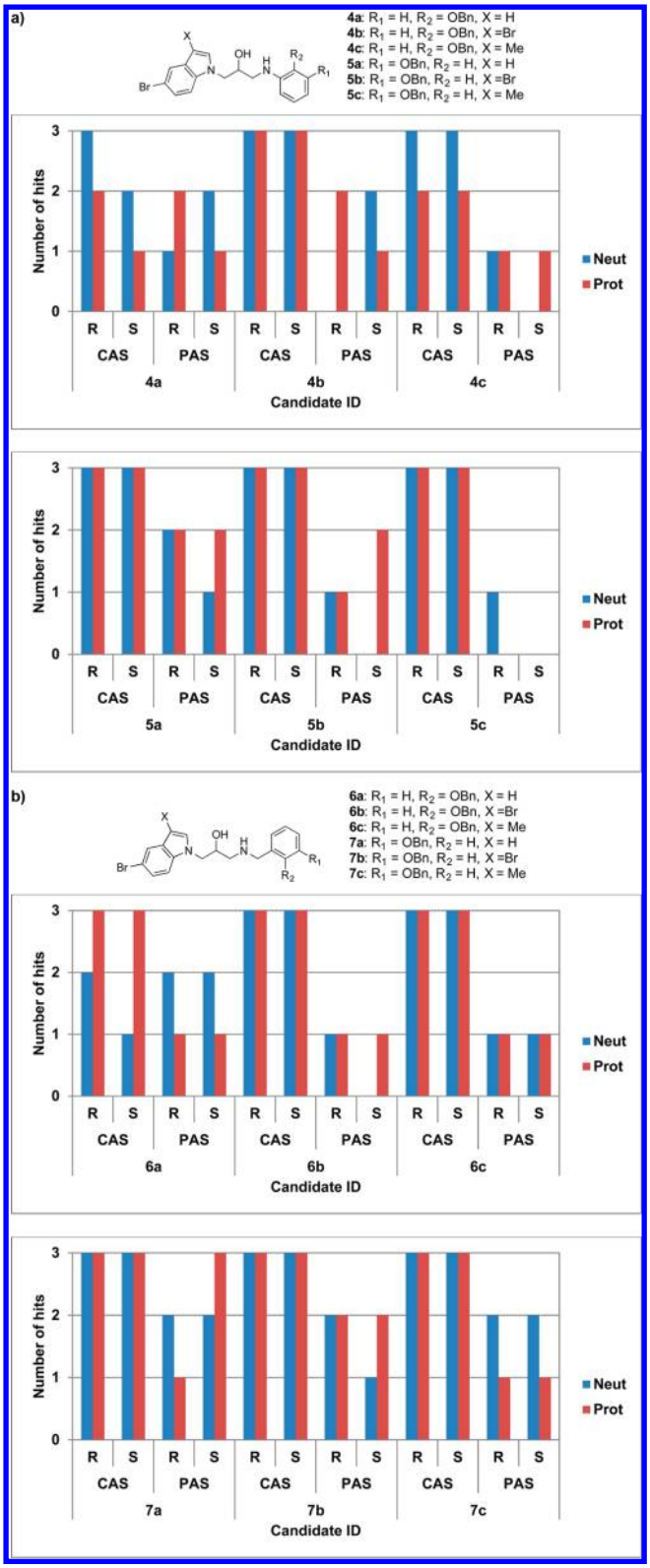

Figure 13. (a) AChE docking results for indole-bearing compounds with (top) ortho- and (bottom) meta-substituted anilines. (b) AChE docking results for indole-bearing compounds with (top) ortho- and (bottom) meta-substituted benzylamines.

DOI: 10.1021/ci500555g
J. Chem. Inf. Model. 2015, 55, 135−148

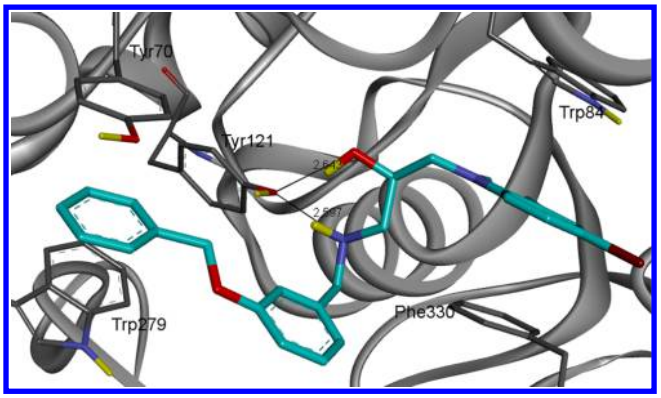

Figure 14. Pose for ligand **7a** in which the indole fragment interacts (through π stacking) with residues Trp 84 and Phe 330 in the CAS, while the treminal Bn group interacts with Tyr 70 and Trp 279 at the PAS site.

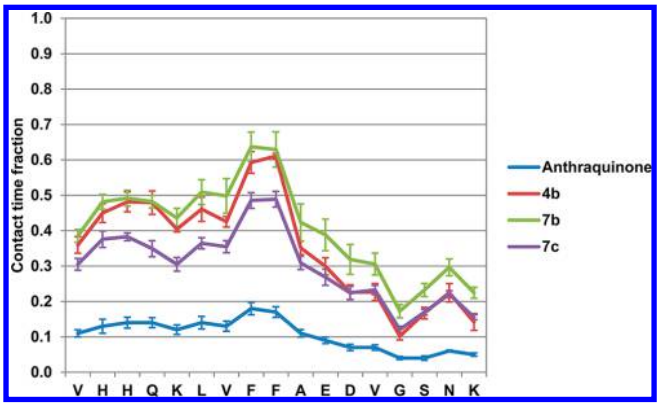

Figure 15. Ligand–peptide residue contact time fractions. The cutoff distance was set at 4.5 Å.

11 and S4) indicates that these compounds clearly interrupt the formation of the hairpin structures that are the hallmark of Aβ peptide aggregates, indicating that these ligands may inhibit amyloid aggregation. Finally, we predict that the benzylamine-containing compounds (**7b** and **7c**) reduce the formation of turns (around the DVSG segment) more efficiently than the aniline-based compound (**4b**).

2.4. Synthesis and Experimental Assays for Indole-Containing Compounds. The indole derivatives whose structures contain an aniline or benzylamine fragment were obtained by the same synthetic route as the carbazole-containing compounds, as indicated in Scheme 2, which includes the list of synthesized molecules.

The results of the binding assays to BACE-1, AChE, and BuChE for the selected compounds as well as the fibril inhibition assays are listed in Table 3. As shown in this table, the meta-substituted benzylamine compounds display altogether higher activities than the ortho-substituted aniline ones for AChE, a result that validates the predictive power of our in silico protocol presented above. More importantly, the replacement of the carbazole moiety by an indole moiety with a meta-substituted benzylamine led to candidates that bind to *all* of the chosen amyloid cascade targets (BACE-1, amyloid aggregates, and the peripheral site in AChE) as well as to AChE's main site and BuChE, implying also a positive cholinergic effect in AD. Hence, compounds such as **7c** are truly multitarget compounds.

Finally, the results displayed in Tables 2 and 3 also afford us with important structural information about the binding poses of both carbazole- and indole-bearing compounds with the cholinergic targets. For instance compounds **7a**, **7b**, and **7c** bind even better to BuChE than to AChE. This result has structural implications, since these two enzymes are highly homologous in the CAS but BuChE replaces the targeted aromatic residues present in the PAS of AChE by nonaromatic ones, precluding the formation of possible π-stacking interactions in this enzyme.[36] Hence, the fact that there are ligands that bind to both cholinesterases may mean that they are able to diffuse to the CAS site in AChE and bind to it. These experimental results support the idea that our design has produced dual AChE inhibitors that bind both to the CAS and the PAS of this enzyme, a conclusion reached as well by the pose search in our docking-based screening simulations (see Figures 13 and 14).

■ DISCUSSION AND CONCLUSIONS

As mentioned in the Introduction, the search for single leads for all of the chosen amyloid cascade targets represents a sizable challenge because of the substantial differences in their binding sites. To tackle this issue, we proposed a two-step protocol. In the first step we designed a pharmacophore, built around the knowledge obtained in our lab and others, that includes the interactions with the molecular targets that the candidates should fulfill. The resulting template allows for the automated screening of multiple candidates using programs such as ZINCPharmer.[37] Our search for compounds in bibliographical data sets led us to a group of carbazole-containing compounds with substituted aniline fragments that were previously identified as neuroprotective and neurogenerative compounds in mice.[8]

The second step of our method includes the evaluation and optimization of the initial set of compounds by a computer-assisted protocol that combines docking calculations for the

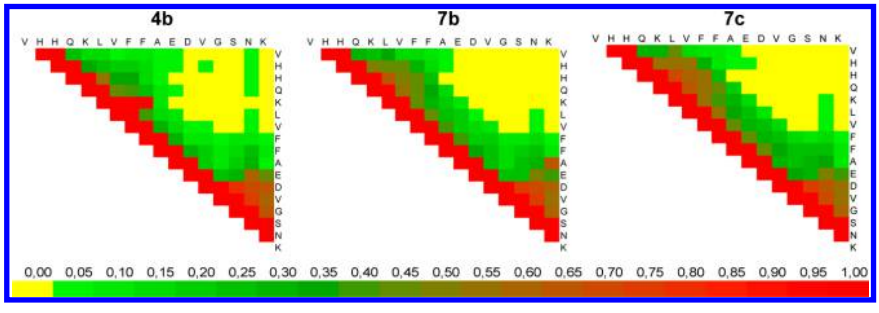

Figure 16. Residue–residue interaction contact maps in the presence of candidates **4b**, **7b**, and **7c**. The cutoff interaction distance was set at 4.5 Å. The color scale shown at the bottom indicates the residence time fractions.

DOI: 10.1021/ci500555g
J. Chem. Inf. Model. 2015, 55, 135–148

Scheme 2. Synthetic Routes and Indole Derivatives Synthesized

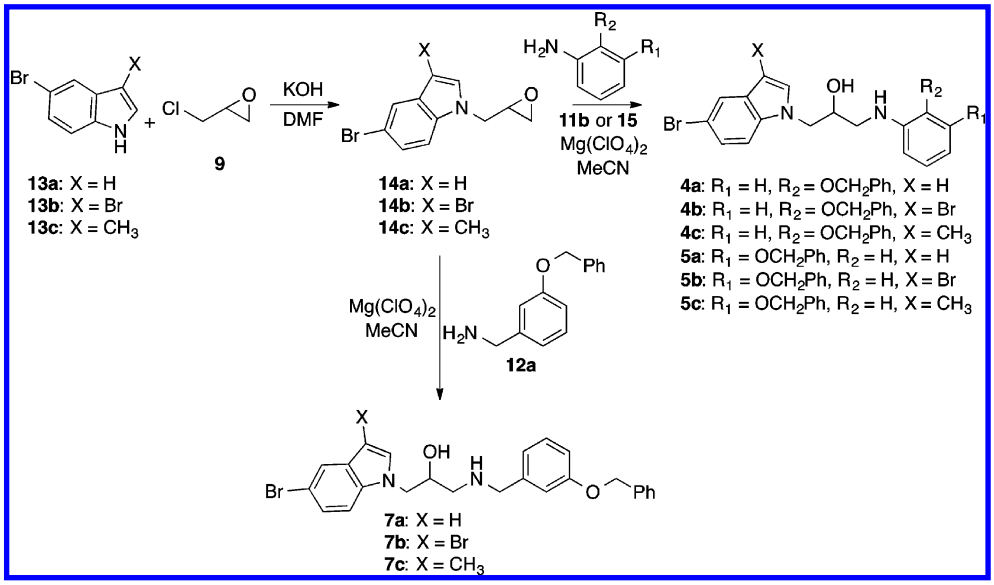

Table 3. Experimental Results for Indole-Based Compounds

	*Ee*AChE		hsBuChE		Aβ(1−40)		BACE-1	
candidate	% Inh. @ 10 μM	IC_{50} (μM)	% Inh. @ 10 μM	IC_{50} (μM)	% Inh. @ 100 μM	IC_{50} (μM)	% Inh. @ 100 μM	IC_{50} (μM)
4a	44 ± 1	–	17 ± 3	–	43 ± 1	–	5.7 ± 1.6	–
4b	45 ± 2	–	18 ± 3	–	23 ± 2	–	6.3 ± 1.4	–
4c	44 ± 1	–	19 ± 1	–	43 ± 5	–	16.4 ± 0.1	–
5a	–	8.5 ± 0.7	20 ± 2	–	55 ± 3	–	3.5 ± 2.4	–
5b	–	9.3 ± 0.6	24 ± 1	–	22 ± 2	–	1.8 ± 0.6	–
5c	–	12 ± 1	17 ± 1	–	57 ± 2	–	0.1 ± 0.1	–
7a	–	10.4 ± 0.1	–	0.70 ± 0.02	57 ± 3	–	–	3.0 ± 1.4
7b	–	9.1 ± 1.1	–	0.29 ± 0.05	47 ± 2	–	–	2.5 ± 0.1
7c	–	5.9 ± 1.0	–	0.39 ± 0.03	–	34 ± 2	–	4.3 ± 0 0.8

enzyme targets (BACE-1 and AChE) with MD simulations for the in silico study of Aβ aggregation inhibition. The results of the docking calculations rely not only on obtaining the best-scoring compounds but more importantly on fulfilling the pattern of interactions with the cardinal residues in our targets as shown in our pharmacophore scheme (see Figure 1). The MD simulations used for amyloid aggregation inhibition studied the time evolution of an amyloid peptide fragment in the presence and absence of our candidates, with the aim of determining the strength of the binding to "hot spot" peptide fragments as well as understanding and evaluating the effect of the candidates on the peptide secondary structure.

Our computer-aided protocol was used with a twofold aim: (1) to investigate whether the original compounds owed their known biological activity to their binding to some of the amyloid cascade targets and (2) to search for analogues with increased affinities for the largest possible group of amyloid cascade targets. The first round of calculations on our original compounds (that purportedly had neuroprotective and neurogenerative properties) displayed very few hits in BACE-1 (see Figure 5) but a number of hits in AChE. Our binding assays (Table 2) corroborated the outcome of our calculations, since the initial set of compounds displayed low affinities for BACE-1 (not surpassing 4% BACE-1 inhibition at 100 μM). Nevertheless, as predicted by our calculations, micromolar affinity for AChE was exhibited by those compounds presenting the largest scoring function values in our docking calculations (see the results for **1e** and **1f** in Figure 7). Perusal of the exit docking poses indicates that these compounds are able to span the two AChE binding sites, a result that could explain their better affinity compared with their congeners. Finally, some of the compounds in the initial set displayed fibril formation inhibition slightly above that of the reference compound 9,10-anthraquinone.[35]

In order to improve the binding across the amyloid targets and especially for BACE-1, we proceeded to modify these compounds with the information afforded by two computer-aided design cycles. The initial screening results for BACE-1 anticipated that most of the hits were obtained with the protonated amino group in the aniline (see Figure 5). In order to increase the probability that the amino group would actually be protonated, we replaced the aniline moiety by a benzylamine fragment. The docking results predicted that the second-generation compounds should have improved hit rates mainly for BACE-1. In order to test this outcome, we synthesized and assayed two of the benzylamine-containing compounds that showed promising results in the docking calculations (**3e** and **3f**). The binding assays indicated that the new candidates had improved binding affinities for BACE-1 by more than 3 orders of magnitude (IC_{50} = 3.1 μM). Interestingly enough, these compounds also showed affinity for BuChE. In healthy brains, AChE hydrolyzes about 80% of acetylcholine while BuChE plays a secondary role. However, as AD progresses, the activity of AChE is greatly reduced in specific brain regions while the BuChE activity increases, likely as a compensation for the AChE

DOI: 10.1021/ci500555g
J. Chem. Inf. Model. 2015, 55, 135−148

depletion.[38] Consequently, both enzymes are useful therapeutic targets for AD, and our experimental results indicate that our compounds not only should affect the amyloid cascade at the core of AD but also should have a positive cholinergic effect.[38]

The design of the third-generation ligands was afforded by the inspection of the exiting poses of the carbazole-containing compounds, which showed that there were some steric clashes between the carbazole moiety and some of the residues belonging either to BACE-1 or AChE (see Figures S1 and S2). In order to avoid close van der Waals overlaps, we designed a new set of ligands in which the carbazole moiety was replaced by indole, a smaller fragment, while at the other end we kept the substituted aniline or benzylamine fragments. Even in the case of the aniline-containing compounds, the replacement of a carbazole by an indole (see Figures 5 and 12) substantially increases the number of hits for BACE-1, especially when the ligand is neutral. Moreover, we predict that an additional hit enrichment could be obtained by replacing the aniline moiety by a benzylamine fragment substituted at the meta position rather than at the ortho position (see Table S7 and Figure 12). Our docking calculations show that AChE has a very similar inhibitor preference as BACE-1, meaning that a consensus inhibitor design for the two enzymes has been reached.

A sizable effort has been devoted to understanding the effect of ligands on the secondary structure of Aβ peptides by MD simulations in order to gain some insight into the inhibitory effect of these ligands.[28] For instance, Wang et al.[39] studied the time evolution of the Aβ peptide in the presence of polyphenolic xanthones. The analysis of rather short MD simulations (in the nanosecond regime) indicated that the presence of these ligands seem to help retain the α-helix secondary structure (from which these simulations started) and hence preclude amyloid aggregation. On the other hand, the results of our calculations shed light on an open question that relates to the existence of an amyloidogenic core that serves as a template for amyloid oligomers and fibril formation, an issue that is relevant not only to AD but also to other pathologies (e.g., type-2 diabetes and Parkinson's disease) that are associated with the misfolding of polypeptides.[40] Hence, a possible paradigm for an Aβ aggregation inhibition route could rely on precluding the emergence of the template structure with a β-hairpin structure (around the DVGS motif) observed in various NMR experiments.[41] Comparison of the results obtained from our MD simulations of an Aβ fragment (residues 12−28) in the presence and absence of our candidate compounds seems to indicate that the best aggregation inhibitors are able to modulate the secondary structure of the peptide, partially precluding the formation of a hairpin aggregation core. Perusal of Figures 10 and 15 indicates that the modulation of the secondary structure of the Aβ peptide is achieved by interaction of the ligand with the pairs of aromatic residues (predominantly Phe19−Phe20) present in the peptide segment studied. It was found that the hydrophobic interactions that involve these aromatic residues are vital for the genesis of the hairpin structure through the collapse of the hydrophobic stretch Leu17−Ala21.[41] The only other aromatic residues present in the full Aβ peptide are single amino acids that are located in the segment comprising the first 11 residues (which is known to lack any structure in peptide aggregates) and hence possibly do not have any role in inducing aggregation. Figure S3 displays a snapshot of the interaction between compound **7b** and the Aβ12−28 peptide as obtained from the MD simulation. As shown in this figure, there is a π-stacking interaction between the aromatic core of the benzylamine fragment and one of the aromatic residues mentioned above.

We calculated the variability, as given by the standard deviation (SD), of the crucial contacts between the segments DVGS and VHHQ in the MD trajectory (see Table S8 for some typical examples). The results show an increase in the SD values in the absence of a ligand, which indicates that the presence of our ligands seems to reduce the contact fluctuations, stabilizing secondary structures other than a turn.

There seems to be some relationship between the disruption of the aforementioned turn in our simulations and the result of the ThT assays. For instance, 9,10-anthraquinone, a compound that results in only 30% inhibition of fibril formation, precludes turn formation to a much lesser extent than some of our best compounds, such as **7c**. Moreover, the indole/aniline derivative **4b** is much less effective in precluding the turn template than the benzylamine analogue **7b**, providing support for our MD simulation results. Nevertheless, we expect that this simple protocol based on MD simulations of a single Aβ peptide fragment may not be able to give a quantitative inhibition ranking but rather would enable us to distinguish the binders from the inactive compounds. Presently we are performing our MD simulations on a larger set of peptide−ligand complexes in order to validate the predictive capabilities of our protocol that could be useful in the design of Aβ aggregation inhibitors.

The results of the enzyme FRET assays for BACE-1, AChE, and BuChE as well as ThT fibril formation assays on indole-based compounds with aniline and meta-substituted benzylamine moieties fully support the outcome of our calculations, indicating that the latter set of compounds (**7a**, **7b**, and **7c**) are by far the most superior candidates, exhibiting highly improved ligand efficiency and displaying multitarget behavior across the amyloid cascade and cholinergic pathways.

Besides affording robust predictions about the relative affinity of our candidate compounds, our computer-assisted protocol has provided us with valuable structural predictions such as the flap opening in BACE-1 when bound to our inhibitors and the orientation of the ligands in AChE, issues we are trying to verify by X-ray crystallography.

■ ASSOCIATED CONTENT

Supporting Information

Additional data for docking to BACE-1 and AChE as well as aggregation simulations as described in the text and general materials and methods for syntheses and in vitro biological evaluations. This material is available free of charge via the Internet at http://pubs.acs.org.

■ AUTHOR INFORMATION

Corresponding Authors

*E-mail: mc.villaverde@usc.es.
*E-mail: fredy.sussman@usc.es.

Notes

The authors declare no competing financial interest.

■ ACKNOWLEDGMENTS

Financial support from the Ministerio de Economia y Competitividad of Spain (Project CTQ2011-22436) and the Xunta de Galicia (CN2011/047 and 10CSA209063PR) is gratefully acknowledged. We thank the Center for Supercomputing in Galicia (CESGA) for computer time and Prof. Amedeo Caflisch for hosting one of us (J.L.D.) for a short-term

DOI: 10.1021/ci500555g
J. Chem. Inf. Model. 2015, 55, 135−148

visit that allowed him to become familiar with the computer simulation protocols used in the study of amyloid aggregation.

REFERENCES

(1) Mangialasche, F.; Solomon, A.; Winblad, B.; Mecocci, P.; Kivipelto, M. Alzheimer's disease: Clinical trials and drug development. *Lancet Neurol.* **2010**, *9*, 702−716.

(2) Walsh, D. M.; Selkoe, D. J. Deciphering the molecular basis of memory failure in Alzheimer's disease. *Neuron* **2004**, *44*, 181−193.

(3) Selkoe, D. J. Preventing Alzheimer's disease. *Science* **2012**, *337*, 1488−1492.

(4) Inestrosa, N. C.; Alvarez, A.; Pérez, C. A.; Moreno, R. D.; Vicente, M.; Linker, C.; Casanueva, O. I.; Soto, C.; Garrido, J. Acetylcholinesterase accelerates assembly of amyloid-β-peptides into Alzheimer's fibrils: Possible role of the peripheral site of the enzyme. *Neuron* **1996**, *16*, 881−891.

(5) (a) Cavalli, A.; Bolognesi, M. L.; Capsoni, S.; Andrisano, V.; Bartolini, M.; Margotti, E.; Cattaneo, A.; Recanatini, M.; Melchiorre, C. A small molecule targeting the multifactorial nature of Alzheimer's disease. *Angew. Chem., Int. Ed.* **2007**, *46*, 3689−3692. (b) Zhu, Y.; Xiao, K.; Ma, L.; Xiong, B.; Fu, Y.; Yu, H.; Wang, W.; Wang, X.; Hu, D.; Peng, H.; Li, J.; Gong, Q.; Chai, Q.; Tang, X.; Zhang, H.; Li, J.; Shen, J. Design, synthesis and biological evaluation of novel dual inhibitors of acetylcholinesterase and β-secretase. *Bioorg. Med. Chem.* **2009**, *17*, 1600−1613. (c) Fernández-Bachiller, M. I.; Pérez, C.; Monjas, L.; Rademann, J.; Rodríguez-Franco, M. I. New tacrine-4-oxo-4*H*-chromene hybrids as multifunctional agents for the treatment of Alzheimer's disease, with cholinergic, antioxidant, and β-amyloid-reducing properties. *J. Med. Chem.* **2012**, *55*, 1303−1317.

(6) Viayna, E.; Gómez, T.; Galdeano, C.; Ramírez, L.; Ratia, M.; Badia, A.; Clos, M. V.; Verdaguer, E.; Junyent, F.; Camins, A.; Pallàs, M.; Bartolini, M.; Mancini, F.; Andrisano, V.; Arce, M. P.; Rodríguez-Franco, M. I.; Bidon-Chanal, A.; Luque, F. J.; Camps, P.; Muñoz-Torrero, D. Novel huprine derivatives with inhibitory activity toward β-amyloid aggregation and formation as disease-modifying anti-Alzheimer drug candidates. *ChemMedChem* **2010**, *5*, 1855−1870.

(7) (a) Bolognesi, M. L.; Cavalli, A.; Valgimigli, L.; Bartolini, M.; Rosini, M.; Andrisano, V.; Recanatini, M.; Melchiorre, C. Multi-target-directed drug design strategy: From a dual binding site acetylcholinesterase inhibitor to a trifunctional compound against Alzheimer's disease. *J. Med. Chem.* **2007**, *50*, 6446−6449. (b) Bolognesi, M. L.; Bartolini, M.; Tarozzi, A.; Morroni, F.; Lizzi, F.; Milelli, A.; Minarini, A.; Rosini, M.; Hrelia, P.; Andrisano, V.; Melchiorre, C. Multitargeted drugs discovery: Balancing anti-amyloid and anticholinesterase capacity in a single chemical entity. *Bioorg. Med. Chem. Lett.* **2011**, *21*, 2655−2658. (c) Li, R.-S.; Wang, X.-B.; Hu, X.-J.; Kong, L.-Y. Design, synthesis and evaluation of flavonoid derivatives as potential multifunctional acetylcholinesterase inhibitors against Alzheimer's disease. *Bioorg. Med. Chem. Lett.* **2013**, *23*, 2636−2641.

(8) MacMillan, K. S.; Naidoo, J.; Liang, J.; Melito, L.; Williams, N. S.; Morlock, L.; Huntington, P. J.; Estill, S. J.; Longgood, J.; Becker, G. L.; McKnight, S. L.; Pieper, A. A.; De Brabander, J. K.; Ready, J. M. Development of proneurogenic, neuroprotective small molecules. *J. Am. Chem. Soc.* **2011**, *133*, 1428−1437.

(9) Yuan, J.; Venkatraman, S.; Zheng, Y.; McKeever, B. M.; Dillard, L. W.; Singh, S. B. Structure-based design of β-site APP cleaving enzyme 1 (BACE1) inhibitors for the treatment of Alzheimer's disease. *J. Med. Chem.* **2013**, *56*, 4156−4180.

(10) Domínguez, J. L.; Christopeit, T.; Villaverde, M. C.; Gossas, T.; Otero, J. M.; Nyström, S.; Baraznenok, V.; Lindström, E.; Danielson, U. H.; Sussman, F. Effect of the protonation state of the titratable residues on the inhibitor affinity to BACE-1. *Biochemistry* **2010**, *49*, 7255−7263.

(11) Sussman, F.; Villaverde, M. C.; Domínguez, J. L.; Danielson, U. H. On the active site protonation state in aspartic proteases: Implications for drug design. *Curr. Pharm. Des.* **2013**, *19*, 4257−4275.

(12) Dvir, H.; Silman, I.; Harel, M.; Rosenberry, T. L.; Sussman, J. L. Acetylcholinesterase: From 3D structure to function. *Chem.-Biol. Interact.* **2010**, *187*, 10−22.

(13) Hopkins, C. R. ACS chemical neuroscience molecule spotlight on dimebon. *ACS Chem. Neurosci.* **2010**, *1*, 587−588.

(14) Yang, W.; Wong, Y.; Ng, O. T. W.; Bai, L.-P.; Kwong, D. W. J.; Ke, Y.; Jiang, Z.-H.; Li, H.-W.; Yung, K. K. L.; Wong, M. S. Inhibition of β-amyloid peptide aggregation by multifunctional carbazole-based fluorophores. *Angew. Chem.* **2012**, *124*, 1840−1846.

(15) *GOLD*, version 5.1; Cambridge Crystallographic Data Centre: Cambridge, U.K..

(16) Jones, G.; Willett, P.; Glen, R. C. Molecular recognition of receptor sites using a genetic algorithm with a description of desolvation. *J. Mol. Biol.* **1995**, *245*, 43−53.

(17) Jones, G.; Willett, P.; Glen, R. C.; Leach, A. R.; Taylor, R. Development and validation of a genetic algorithm for flexible docking. *J. Mol. Biol.* **1997**, *267*, 727−748.

(18) Baxter, C. A.; Murray, C. W.; Clark, D. E.; Westhead, D. R.; Eldridge, M. D. Flexible docking using tabu search and an empirical estimate of binding affinity. *Proteins* **1998**, *33*, 367−382.

(19) Eldridge, M. D.; Murray, C. W.; Auton, T. R.; Paolini, G. V.; Mee, R. P. Empirical scoring functions: I. The development of a fast empirical scoring function to estimate the binding affinity of ligands in receptor complexes. *J. Comput.-Aided Mol. Des.* **1997**, *11*, 425−445.

(20) Verdonk, M. L.; Cole, J. C.; Hartshorn, M. J.; Murray, C. W.; Taylor, R. D. Improved protein−ligand docking using GOLD. *Proteins* **2003**, *52*, 609−623.

(21) Korb, O.; Stützle, T.; Exner, T. E. Empirical scoring functions for advanced protein−ligand docking with PLANTS. *J. Chem. Inf. Model.* **2009**, *49*, 84−96.

(22) Hong, L.; Koelsch, G.; Lin, X.; Wu, S.; Terzyan, S.; Ghosh, A. K.; Zhang, X. C.; Tang, J. Structure of the protease domain of memapsin 2 (β-secretase) complexed with inhibitor. *Science* **2000**, *290*, 150−153.

(23) Wang, Y.-S.; Strickland, C.; Voigt, J. H.; Kennedy, M. E.; Beyer, B. M.; Senior, M. M.; Smith, E. M.; Nechuta, T. L.; Madison, V. S.; Czarniecki, M.; McKittrick, B. A.; Stamford, A. W.; Parker, E. M.; Hunter, J. C.; Greenlee, W. J.; Wyss, D. F. Application of fragment-based NMR screening, X-ray crystallography, structure-based design, and focused chemical library design to identify novel μM leads for the development of nM BACE-1 (β-site APP cleaving enzyme 1) inhibitors. *J. Med. Chem.* **2010**, *53*, 942−950.

(24) Patel, S.; Vuillard, L.; Cleasby, A.; Murray, C. W.; Yon, J. Apo and inhibitor complex structures of BACE (β-secretase). *J. Mol. Biol.* **2004**, *343*, 407−416.

(25) *Discovery Studio*, versions 2.1 and 2.5; Accelrys Inc.: San Diego, CA.

(26) Rydberg, E. H.; Brumshtein, B.; Greenblatt, H. M.; Wong, D. M.; Shaya, D.; Williams, L. D.; Carlier, P. R.; Pang, Y.-P.; Silman, I.; Sussman, J. L. Complexes of alkylene-linked tacrine dimers with *Torpedo californica* acetylcholinesterase: Binding of bis(5)-tacrine produces a dramatic rearrangement in the active-site gorge. *J. Med. Chem.* **2006**, *49*, 5491−5500.

(27) (a) Convertino, M.; Vitalis, A.; Caflisch, A. Disordered binding of small molecules to Aβ(12−28). *J. Biol. Chem.* **2011**, *286*, 41578−41588. (b) Scherzer-Attali, R.; Pellarin, R.; Convertino, M.; Frydman-Marom, A.; Egoz-Matia, N.; Peled, S.; Levy-Sakin, M.; Shalev, D. E.; Caflisch, A.; Gazit, E.; Segal, D. Complete phenotypic recovery of an Alzheimer's disease model by a quinone−tryptophan hybrid aggregation inhibitor. *PLoS One* **2010**, *5*, No. e11101. (c) Scherzer-Attali, R.; Convertino, M.; Pellarin, R.; Gazit, E.; Segal, D.; Caflisch, A. Methylations of tryptophan-modified naphthoquinone affect its inhibitory potential toward Aβ aggregation. *J. Phys. Chem. B* **2013**, *117*, 1780−1789.

(28) Lemkul, J. A.; Bevan, D. R. The role of molecular simulations in the development of inhibitors of amyloid β-peptide aggregation for the treatment of Alzheimer's disease. *ACS Chem. Neurosci.* **2012**, *3*, 845−856.

(29) Lührs, T.; Ritter, C.; Adrian, M.; Riek-Loher, D.; Bohrmann, B.; Döbeli, H.; Schubert, D.; Riek, R. 3D structure of Alzheimer's amyloid-β(1−42) fibrils. *Proc. Natl. Acad. Sci. U.S.A.* **2005**, *102*, 17342−17347.

(30) Brooks, B. R.; Bruccoleri, R. E.; Olafson, B. D.; States, D. J.; Swaminathan, S.; Karplus, M. CHARMM: A program for macro-

DOI: 10.1021/ci500555g
J. Chem. Inf. Model. 2015, 55, 135−148

molecular energy, minimization, and dynamics calculations. *J. Comput. Chem.* **1983**, *4*, 187−217.
(31) Haberthür, U.; Caflisch, A. FACTS: Fast analytical continuum treatment of solvation. *J. Comput. Chem.* **2008**, *29*, 701−715.
(32) Domínguez, J. L.; Villaverde, M. C.; Sussman, F. Effect of pH and ligand charge state on BACE-1 fragment docking performance. *J. Comput.-Aided Mol. Des.* **2013**, *27*, 403−417.
(33) Asso, V.; Ghilardi, E.; Bertini, S.; Digiacomo, M.; Granchi, C.; Minutolo, F.; Rapposelli, S.; Bortolato, A.; Moro, S.; Macchia, M. α-Naphthylaminopropan-2-ol derivatives as BACE1 inhibitors. *ChemMedChem* **2008**, *3*, 1530−1534.
(34) Paleo, M. R.; Aurrecoechea, N.; Jung, K.-Y.; Rapoport, H. Formal enantiospecific synthesis of (+)-FR900482. *J. Org. Chem.* **2003**, *68*, 130−138.
(35) Convertino, M.; Pellarin, R.; Catto, M.; Carotti, A.; Caflisch, A. 9,10-Anthraquinone hinders β-aggregation: How does a small molecule interfere with Aβ-peptide amyloid fibrillation? *Protein Sci.* **2009**, *18*, 792−800.
(36) Nicolet, Y.; Lockridge, O.; Masson, P.; Fontecilla-Camps, J. C.; Nachon, F. Crystal structure of human butyrylcholinesterase and of its complexes with substrate and products. *J. Biol. Chem.* **2003**, *278*, 41141−41147.
(37) Koes, D. R.; Camacho, C. J. ZINCPharmer: Pharmacophore search of the ZINC database. *Nucleic Acids Res.* **2012**, *40*, W409−W414.
(38) Li, S.-Y.; Jiang, N.; Xie, S.-S.; Wang, K. D. G.; Wang, X.-B.; Kong, L.-Y. Design, synthesis and evaluation of novel tacrine−rhein hybrids as multifunctional agents for the treatment of Alzheimer's disease. *Org. Biomol. Chem.* **2014**, *12*, 801−814.
(39) Wang, Y.; Xia, Z.; Xu, J.-R.; Wang, Y.-X.; Hou, L.-N.; Qiu, Y.; Chen, H.-Z. α-Mangostin, a polyphenolic xanthone derivative from mangosteen, attenuates β-amyloid oligomers-induced neurotoxicity by inhibiting amyloid aggregation. *Neuropharmacology* **2012**, *62*, 871−881.
(40) Buchanan, L. E.; Dunkelberger, E. B.; Tran, H. Q.; Cheng, P.-N.; Chiu, C.-C.; Cao, P.; Raleigh, D. P.; de Pablo, J. J.; Nowick, J. S.; Zanni, M. T. Mechanism of IAPP amyloid fibril formation involves an intermediate with a transient β-sheet. *Proc. Natl. Acad. Sci. U.S.A.* **2013**, *110*, 19285−19290.
(41) Ahmed, M.; Davis, J.; Aucoin, D.; Sato, T.; Ahuja, S.; Aimoto, S.; Elliot, J. I.; Van Nostrand, W. E.; Smith, S. O. Structural conversion of neurotoxic amyloid-β_{1-42} oligomers to fibrils. *Nat. Struct. Mol. Biol.* **2010**, *17*, 561−567.

DOI: 10.1021/ci500555g
J. Chem. Inf. Model. 2015, 55, 135−148